

Indium Single-Ion Optical Frequency Standard

Thomas Becker^{1,2}, Mario Eichenseer^{1,2}, Alexander Yu. Nevsky^{1,3},
Ekkehard Peik^{1,2}, Christian Schwedes^{1,2}, Mikhail N. Skvortsov^{1,3},
Joachim von Zanthier^{1,2}, and Herbert Walther^{1,2}

¹ Max-Planck-Institut für Quantenoptik

Hans-Kopfermann-Str. 1, 85748 Garching, Germany

² Sektion Physik der Ludwig-Maximilians-Universität, München, Germany

³ permanent address: Institute of Laser Physics, 630090 Novosibirsk, Russia

Abstract. We are investigating the $5s^2\ ^1S_0 \rightarrow 5s5p\ ^3P_0$ transition of a single trapped laser-cooled $^{115}\text{In}^+$ ion as a candidate for an optical frequency standard. This line with a natural linewidth of only 0.8 Hz is highly immune to systematic frequency shifts. For sideband laser cooling and fluorescence detection of the indium ion the $5s^2\ ^1S_0 \rightarrow 5s5p\ ^3P_1$ transition at 230.6 nm is excited. Temperatures below 100 μK and a mean vibrational quantum number $\langle n \rangle < 1$ of the ion in the trap have been reached. For the clock transition a resolution of $1.3 \cdot 10^{-13}$ (linewidth 170 Hz) has been obtained so far, limited by the short term frequency fluctuations of the clock laser. The absolute frequency of the $^1S_0 \rightarrow ^3P_0$ transition was measured by making a link to the reference frequency of the methane-stabilised HeNe laser using a frequency chain.

1 Introduction

A single laser-cooled ion in a radiofrequency trap represents a good approximation to the spectroscopic ideal of a motionless point-like absorber in a perturbation-free environment. It is consequently regarded as a perfect system for an optical atomic clock of very high accuracy [1,2]. With a frequency-stable laser locked to a narrow absorption resonance of a trapped ion a stability $\sigma_y(1\text{ s}) = 10^{-15}$ and an accuracy of a few times 10^{-18} seem possible. High-resolution spectroscopy of forbidden optical transitions has yielded sub-kHz linewidths in Hg^+ [3], Ba^+ [4], Sr^+ [5], Yb^+ [6] and In^+ . In the first four alkali-like ions, quadrupole transitions between S and D states are investigated. We are studying the earth-alkali-like spectrum of In^+ [7], where the lowest two levels $5s^2\ ^1S_0$ and $5s5p\ ^3P_0$ are connected by a hyperfine-induced electric dipole transition at a wavelength of 236.5 nm which has a natural linewidth of only 0.8 Hz. Figure 1 shows the relevant energy levels of In^+ .

As a candidate for a primary optical frequency standard In^+ has three main advantages:

(i) Since the electronic angular momenta in both states of the clock transition $^1S_0 \rightarrow ^3P_0$ vanish, the shifts of the transition frequency due to external electric or magnetic fields are very small. In fact, the 3P_0 state is not a pure $J = 0$ state but contains small hyperfine admixtures of the $5s5p$ levels 3P_1 and 1P_1 . These perturbations are responsible for the non-vanishing electric dipole moment

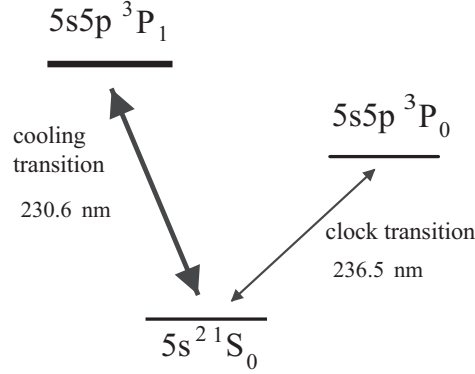


Fig. 1. The lowest energy levels of the In^+ ion

between this state and the ground state [7]. Possible systematic shifts of the clock transition frequency will be discussed in Section 3.

(ii) To excite the clock transition a reliable and frequency-stable laser source is required – a problem that becomes especially demanding as shorter wavelength in the ultraviolet are required. The In^+ transition has the advantage that it coincides with the fourth harmonic of the 946 nm laser line of Nd:YAG. The availability of this diode-laser-pumped solid-state laser is of significance for long-term operation of the optical frequency standard. The measurements described here are done with a conventional setup made from discrete optical elements [8,9], but we have recently completed the construction of a second clock laser system based on a monolithic ring-laser [10,11]. This compact laser design offers very high intrinsic stability, which facilitates the lock onto an external reference cavity.

(iii) Laser cooling of In^+ is performed by using the narrow intercombination line $5s^2 \ ^1S_0 \rightarrow 5s5p \ ^3P_1$. With a natural linewidth of 360 kHz, the photon scattering rate on this transition is sufficiently high to detect a single ion via the resonance fluorescence. At the same time the line is narrow enough to allow resolution of the ≈ 1 MHz vibrational frequencies of the ion in the trap. In this parameter regime, sideband cooling [1,12,13] allows the ion to be cooled to the motional ground state of the trap. We have used a bichromatic sideband cooling method to increase the cooling efficiency at higher temperatures. Ground state cooling has been demonstrated for single In^+ ions as well as for two-ion Coulomb crystals. The temperatures that we have reached are below 100 μK [14].

2 High-Resolution Spectroscopy and Absolute Frequency Measurement of the Clock Transition

The ion is trapped in a quadrupole radiofrequency trap that is a geometrical variant of the original Paul trap and basically consists of only a ring electrode

(Paul-Straubel trap [15,16]). This type of trap is relatively simple to fabricate in miniature size (1 mm diameter of the ring), making it easy to confine the ion to a region in space that is smaller than the optical wavelength (Lamb-Dicke regime). It is also a geometrically quite open structure that allows good optical access to the trapped ion. The trap is driven with a RF field at 10 MHz; the oscillation frequencies in the time-averaged pseudopotential are 1.4 MHz in the axial and 0.9 MHz in the radial direction.

Spectroscopy of the narrow $^1S_0 \rightarrow ^3P_0$ line is performed in optical-optical double resonance using Dehmelt's idea of electron shelving [1]: An excitation of the metastable 3P_0 level leads to a dark period in the single-ion fluorescence signal on the cooling transition until the state decays or the valence electron is brought back to the ground state by a stimulated process. This method leads to strong quantum amplification (absorption of one photon prevents subsequent scattering of some 10^5 to 10^6 photons) and allows detection of transitions to the metastable state with practically 100% efficiency.

The laser system used for excitation of the $^1S_0 \rightarrow ^3P_0$ resonance is described in [9]. It consists of a diode-pumped Nd:YAG laser emitting at 946 nm. This laser contains all the necessary tuning elements and is frequency-stabilised to a passive resonator of high finesse. A second diode-pumped Nd:YAG laser is used for power amplification and efficient generation of the second harmonic at a wavelength of 473 nm. It is a ring laser, containing only a Nd:YAG crystal and a KNbO₃ crystal for frequency doubling. Infrared light from the stable master laser is coupled into this laser to transfer the frequency stability via injection locking. The blue light is coupled into an enhancement cavity to generate the UV radiation at 236.5 nm with a BBO crystal.

In order to obtain high-resolution spectra of the clock transition any light shift and line broadening by the cooling laser have to be avoided. Both laser beams are applied alternately and blocked by means of mechanical shutters. After a clock-laser pulse of 20 ms duration the cooling laser is turned on and the fluorescence photons are counted in a 40 ms time interval. If the count rate corresponds to the single-ion fluorescence level, the excitation attempt of the clock transition is regarded as unsuccessful and repeated either at the same or at a different frequency of the clock laser. If the ion is not fluorescing one excitation of the clock transition is registered and the cooling laser is kept switched on to wait for the decay of the metastable state (lifetime 195 ms). Typically, the frequency of the clock-laser radiation is changed in steps of 8 Hz.

A high-resolution spectrum of the clock transition is shown in Fig. 2. The clock-laser power was reduced to 30 nW to avoid saturation broadening. The fit with a lorentzian curve results in a linewidth of 170 Hz (FWHM), corresponding to a fractional resolution $\delta\nu/\nu$ of $1.3 \cdot 10^{-13}$. A spectral window of 200 Hz width contains 50% of all excitations. According to our present experimental control of the ion temperature, electromagnetic fields and vacuum conditions, no significant Doppler, Zeeman, Stark or collisional broadening of the absorption spectrum of the ion is expected beyond the level of 1 Hz. The linewidth is determined by the frequency instability of the laser and the lineshape is not exactly lorentzian

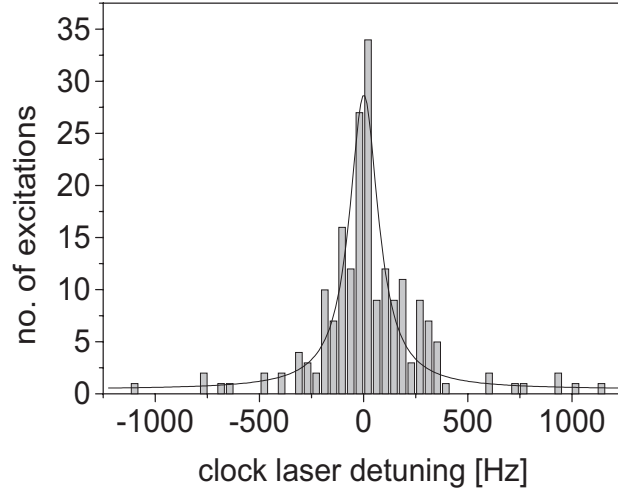


Fig. 2. Excitation spectrum of the $^1S_0 \rightarrow ^3P_0$ resonance of a single indium ion obtained in optical-optical double resonance using electron shelving. The linewidth of the fitted lorentzian is 170 Hz FWHM. The average excitation probability in the peak is about 10% and the total measuring time was 30 minutes

but reflects the fluctuations of the laser frequency, that arise mainly at low modulation frequencies in the range 1-15 Hz. A measurement of the frequency stability of the laser using a second independent high-finesse optical cavity gives a consistent result. Improvements of the vibrational isolation of the reference cavity that is used for the frequency stabilization will probably enable us to resolve the natural linewidth of the ion (0.82 Hz), leading to a resolution of $6 \cdot 10^{-16}$.

Realisation of an optical clock requires first of all a narrow and stable resonance – as is the case for a trapped indium ion – and, secondly, precise frequency determination in comparison with the cesium clock. We have performed two measurements of the absolute frequency of the $^{115}\text{In}^+ 5s^2 ^1S_0 \rightarrow 5s5p ^3P_0$ clock transition, finally reaching an accuracy of 1.8 parts in 10^{13} [17,18,19]. In the last measurement the frequency of the indium clock transition has been compared to a methane-stabilized He-Ne laser at $3.39 \mu\text{m}$ [20] which has been calibrated against an atomic cesium fountain clock [21]. A frequency gap of 37 THz at the fourth harmonic of the He-Ne standard was bridged by a frequency comb generated by a mode locked femtosecond laser [22]. The frequency of the In^+ clock transition was determined to $1\,267\,402\,452\,899.92$ (0.23) kHz where the accuracy is limited by the uncertainty of the He-Ne laser reference. This result represents now the most accurate measurement of an optical transition in a single ion. We are planning to perform a direct measurement against a cesium clock using the new femtosecond laser frequency comb [19]. An interesting prospect afforded by this work is the possibility of linking the clock transition of the indium ion with

the narrow $1S \rightarrow 2S$ resonance of atomic hydrogen [23] and using the high precision of this frequency comparison in a search for temporal variations of the fine-structure constant [24,25,26].

3 Uncertainties of the Indium Standard

In this section we want to estimate the foreseeable systematic line shifts of the atomic reference in an indium frequency standard and compare indium to the alkali-like candidate ions like mercury, ytterbium, barium or strontium that rely on electric quadrupole transitions of the type $S_{1/2} \rightarrow D_{5/2}$. Line shifts may be caused by the motion of the ion, by electric and magnetic fields, by radiation or by collisions. Values for the shifts will be given as $\delta\nu/\nu$, relative to the In^+ transition frequency of $\nu = 1267$ THz.

3.1 Doppler Effect

The motion of the ion in the RF trap can be decomposed into sinusoidal oscillations at (up to three) secular frequencies ω_i and the driving frequency of the trap Ω (micromotion). Usually $\omega_i \ll \Omega$ holds; in our case $\omega/2\pi \approx 1$ MHz and $\Omega/2\pi = 10$ MHz. The motion of the ion leads to frequency modulation sidebands in the absorption and emission spectra. However, since the natural linewidth of the clock transition γ and the recoil frequency $\omega_{rec} = \hbar k^2/2m$ (where $k = 2\pi/\lambda$) are much smaller than ω_i , the sidebands are well resolved, and the carrier is recoil-free and free from the first order Doppler effect. The relativistic second order Doppler effect leads to a shift of the carrier of $\delta\nu/\nu = \langle v^2 \rangle / 2c^2$ where $\langle v^2 \rangle$ is the mean squared velocity of the ion. The squared velocity at temperature T is $\langle v^2 \rangle = 3k_B T/m$ and for In^+ at $T = 100$ μK we find $\delta\nu/\nu = 1.2 \cdot 10^{-19}$. In the quantum ground state of motion $\delta\nu/\nu = \hbar\omega/mc^2 = 4 \cdot 10^{-20}$ for $\omega/2\pi = 1$ MHz. In the ideal RF trap the time averaged kinetic energies of the secular and of the micromotion are equal. Static electric stray fields may, however, displace the ion from the center of the trap and in this case the kinetic energy of the micromotion can be higher than $k_B T$ where T is the temperature of the secular motion. By applying static compensation voltages, this additional micromotion can be minimised and amplitudes below $\Delta x = \lambda/20$ are routinely achieved [14]. In this case the contribution to the second order Doppler effect is $\Delta x^2 \Omega^2 / 8\pi^2 c^2 = 7 \cdot 10^{-20}$. The temperature limits for Doppler cooling of the alkali-like ions are not as low as the temperature achievable with sideband cooling in indium, but the motional line shifts should be well below 10^{-17} in all of these ions.

3.2 Electric Fields

In the RF trap the ion is exposed to an inhomogeneous and time dependent electric field. At each point in the trap the time average of the field vanishes, but the time averaged square of the field is proportional to the squared distance from the trap center. For an ion oscillating around the trap center the

quadratic Stark effect will consequently lead to frequency modulation sidebands and also to a shift of the resonance frequency. Presently, precise data on the polarisabilities of the In^+ levels are not available, but an order of magnitude estimate of the effect is possible: both levels of the clock transition have electronic angular momentum $J = 0$ and are subject to a scalar quadratic Stark shift. The ground state polarisability of the cadmium atom, which is isoelectronic to In^+ , is $\alpha = 8 \cdot 10^{-40} \text{ J}/(\text{V}/\text{m})^2$ [27], leading to a quadratic Stark shift of the ground state of $\alpha/2\hbar = 6 \text{ mHz}/(\text{V}/\text{cm})^2$. The polarisability of In^+ will be smaller than in Cd because the valence electrons are more tightly bound. In helium-like systems the polarisabilities are reduced by a factor 5.5 in going from nuclear charge $Z = 2$ to $Z = 3$ [28]. The polarisability of the $\text{In}^+ 5s5p \ ^3P_0$ level will be comparable to that of $\ ^1S_0$ since both states practically are ground states of the singlet and the triplet system respectively and have strong electric dipole matrix elements only with levels that lie energetically significantly higher: the ground state with the $5s5p \ ^1P_1$ level (at 63033 cm^{-1}) and with the $5s5p \ ^3P_1$ level (at 43349 cm^{-1}), the $5s5p \ ^3P_0$ level mainly with the $5s6s \ ^3S_1$ level (51644 cm^{-1} higher). The quadratic Stark shift of the $\ ^1S_0 \rightarrow \ ^3P_0$ resonance should consequently be well below $1 \text{ mHz}/(\text{V}/\text{cm})^2$. Confinement of the ion in the RF trap relies on the pseudopotential that is proportional to the square of the electric field amplitude. An ion with thermal energy $k_B T$ experiences an average quadratic field strength $\langle E^2 \rangle = 2m\Omega^2 k_B T / e^2$. With typical parameters for In^+ ($T = 100 \text{ } \mu\text{K}$, $\Omega = 2\pi \cdot 10 \text{ MHz}$) we find that the quadratic Stark shift caused by the trap should be smaller than $8 \text{ } \mu\text{Hz}$ or $\delta\nu/\nu < 6 \cdot 10^{-21}$. Static stray fields that displace the ion in the pseudopotential can lead to an extra contribution of $\langle E^2 \rangle$ that is proportional to the square of the displacement (the contribution of the static field is negligible). For a displacement of less than $\lambda/4$ (equivalent to a micromotion amplitude of $\lambda/20$) this additional Stark shift is less than $4 \cdot 10^{-20}$ for our typical trap parameters.

For the alkali-like ions the conditions concerning the Stark shift are slightly less favourable. The metastable $J = 5/2$ level is split into three components by the electric field. Since the energy levels lie energetically closer together, the polarisabilities are higher. A measurement has been performed in the case of Ba^+ and shifts of the three components of the $S_{1/2} \rightarrow D_{5/2}$ resonance between $6 \text{ mHz}/(\text{V}/\text{cm})^2$ and $12 \text{ mHz}/(\text{V}/\text{cm})^2$ have been found [4].

Besides the quadratic Stark shift the alkali-like ions will also show a shift due to the coupling of the quadrupole moment of the D state with electric field gradients. Energy levels with $J > 1/2$ will be split depending on the modulus of the m_J quantum number. In the case of mercury in a linear RF trap quadrupole shifts between $+12 \text{ Hz}$ and -27 Hz have been measured [3]. In a spherical trap no static field gradients are needed for trapping, but gradients of stray fields might be difficult to control. It is thus a considerable advantage of In^+ that both $J = 0$ levels of the clock transition are not influenced by this effect.

3.3 Magnetic Fields

In In^+ hyperfine mixing between the $5s5p$ levels 3P_0 , 3P_1 and 1P_1 is responsible for the non zero electric dipole transition matrix element between 1S_0 and 3P_0 . For the same reason there is a small difference between the g -factors of 1S_0 and 3P_0 [7]. This leads to a symmetric linear Zeeman splitting of the clock transition which we measured to be $\pm 224 \text{ Hz/G}$ for the two $m_F = \pm 1/2 \rightarrow m_F = \pm 1/2$ Zeeman components. There are two possible strategies to deal with this problem: (i) to apply a static field of about 20 mG to split the two lines, to determine both resonances and to interpolate the position of the field free resonance as the mean value of the two frequencies. In this procedure, uncertainties will be introduced by drifts of the magnetic field or of the laser frequency during the time it takes to scan over both resonances. (ii) To eliminate all magnetic fields as precisely as possible and to use the then overlapping resonances. Any uncertainty in the magnetic field will lead to a broadening or an asymmetric line shape. If the field can be controlled to $B = 0 \pm 10 \mu\text{G}$, as is it possible with a three-layer μ -metal shield, the resulting frequency uncertainty will be $1.8 \cdot 10^{-18}$. This will be the dominant source of uncertainty in the indium frequency standard.

In the alkali-like ions the $m_J = \pm 1/2 \rightarrow m_J = \pm 1/2$ components of the $S \rightarrow D$ transitions in even isotopes without nuclear spin show a linear Zeeman shift of the order of 500 kHz/G. It is therefore advisable to work with an isotope with half-integer nuclear spin, so that a linearly field independent transition $m_F = 0 \rightarrow m_F = 0$ becomes available, as has been done in mercury [3] and ytterbium [6]. In this case, however, it is more complicated to obtain cycling transitions for laser cooling and to avoid optical pumping into dark Zeeman or hyperfine states. In these experiments so far a small magnetic guiding field B_0 was applied, which then leads to a linear sensitivity of the resonance frequency to changes of the magnetic field: $\delta\nu \propto B_0\delta B$. In the ytterbium experiment the slope was $\delta\nu/\delta B = 2.6 \text{ kHz/G}$ [6].

3.4 Light Shifts

The cooling laser is close to saturating the $^1S_0 \rightarrow ^3P_1$ transition and can cause a light shift of several hundred kHz. During the interrogation of the clock resonance it has to be blocked with a mechanical shutter and care must be taken to avoid stray light from reaching the trap. Since the trap and the vacuum chamber are held at room temperature, the ion is exposed to blackbody radiation with an average quadratic electric field strength of $\langle E^2 \rangle = 69.2 (\text{V/cm})^2 (T/300 \text{ K})^4$. At 300 K the spectrum of black-body radiation has its peak spectral density at a wavelength of $9 \mu\text{m}$, whereas both, the ground state and the metastable 3P_0 level of In^+ have strong electric-dipole-allowed transitions to the next-higher-lying states only at VUV wavelengths (159 nm and 194 nm, respectively). Consequently, the influence of the thermal radiation can be estimated by using the static polarisabilities. While the total blackbody AC Stark shift might be of the order of $5 \cdot 10^{-17}$, control of the temperature to $300 \pm 1 \text{ K}$ will be found sufficient to reduce the uncertainty in the shift to $7 \cdot 10^{-19}$. Again, the level scheme of

In^+ turns out to be more favourable than the alkali-like spectra, for the reasons already mentioned in Section 3.2.

Precise data on the collisional shifts in In^+ are presently not available and an estimate can only be based on data from comparable atomic systems. Assuming a shift coefficient of $10^{-10} \text{ cm}^3/\text{s}$ and ultrahigh vacuum conditions ($5 \cdot 10^{-8} \text{ Pa}$), the collisional frequency shift would be $1 \cdot 10^{-18}$.

Table 1 presents the summary of the estimated uncertainties, showing that the indium frequency standard should be able to provide an accuracy of a few parts in 10^{18} , making this system a most promising candidate for a future primary optical clock.

Table 1. Estimated shifts and uncertainties of the indium frequency standard. All values are given relative to the frequency 1267 THz. For the small effects the uncertainties may be comparable to the total shift, with the exception of the blackbody AC stark shift. All Stark shifts are based on an estimated upper bound for the polarisability. The collisional shift is an estimate based on data in comparable atomic systems. The assumed conditions are: $T_{ion} = 100 \text{ } \mu\text{K}$; uncompensated stray fields, leading to micro-motion amplitude $< \lambda/20 = 12 \text{ nm}$; $\Delta B = 10 \text{ } \mu\text{G}$; $P = 5 \cdot 10^{-8} \text{ Pa}$; $T_{trap} = 300 \text{ K} \pm 1 \text{ K}$

effect	shift	uncertainty
quadratic Doppler effect (thermal)	$1.2 \cdot 10^{-19}$	
" (through stray fields)	$7 \cdot 10^{-20}$	
quadratic Stark shift of trap (thermal)	$6 \cdot 10^{-21}$	
" (through stray fields)	$4 \cdot 10^{-20}$	
linear Zeeman effect	$1.8 \cdot 10^{-18}$	
blackbody AC Stark shift	$5 \cdot 10^{-17}$	$7 \cdot 10^{-19}$
collisions	$1 \cdot 10^{-18}$	

Acknowledgments

We gratefully acknowledge the collaboration with R. Holzwarth, J. Reichert, Th. Udem, Th. Hänsch and S. N. Bagayev in the absolute optical frequency measurement.

References

1. H. Dehmelt: IEEE Trans. Instrum. Meas. **31**, 83 (1982)

2. For a recent review see: A. A. Madej and J. E. Bernard: in 'Frequency Measurement and Control: Advanced Techniques and Future Trends', Springer Topics in Applied Physics, Ed.: A. N. Luiten (Springer, Berlin, 2000) pp. 149–190
3. R. J. Rafac, B. C. Young, J. A. Beall, W. M. Itano, D. J. Wineland, and J. C. Bergquist: Phys. Rev. Lett. **85**, 2462 (2000)
4. N. Yu, X. Zhao, H. Dehmelt, and W. Nagourney: Phys. Rev. A **50**, 2738 (1994)
5. J. E. Bernard, L. Marmet, and A. Madej: Opt. Commun. **150**, 170 (1998)
6. C. Tamm, D. Engelke, and V. Bühner: Phys. Rev. A **61**, 053405 (2000)
7. E. Peik, G. Hollemann, and H. Walther: Phys. Rev. A **49**, 402 (1994)
8. G. Hollemann, E. Peik, and H. Walther: Opt. Lett. **19**, 192 (1994)
9. G. Hollemann, E. Peik, A. Rusch, and H. Walther: Opt. Lett. **20**, 1871 (1995)
10. Th. J. Kane and R. L. Byer: Opt. Lett. **10**, 65 (1985)
11. I. Freitag, R. Henking, A. Tünnermann, and H. Welling: Opt. Lett. **20**, 2499 (1995)
12. D. J. Wineland and W. M. Itano: Phys. Rev. A **20**, 1521 (1979)
13. F. Diedrich, J. C. Bergquist, W. M. Itano, and D. J. Wineland: Phys. Rev. Lett. **62**, 403 (1989)
14. E. Peik, J. Abel, Th. Becker, J. v. Zanthier, and H. Walther: Phys. Rev. A. **60**, 439 (1999)
15. N. Yu, W. Nagourney, and H. Dehmelt: J. Appl. Phys **69**, 3779 (1991)
16. C. Schrama, E. Peik, W. W. Smith, and H. Walther: Opt. Commun. **101**, 32 (1993)
17. J. v. Zanthier, J. Abel, Th. Becker, M. Fries, E. Peik, H. Walther, R. Holzwarth, J. Reichert, Th. Udem, T. W. Hänsch, A. Yu. Nevsky, M. N. Skvortsov, and S. N. Bagayev: Opt. Commun. **166**, 57 (1999)
18. J. v. Zanthier, Th. Becker, M. Eichenseer, A. Yu. Nevsky, Ch. Schwedes, E. Peik, H. Walther, R. Holzwarth, J. Reichert, Th. Udem, T. W. Hänsch, P. V. Pokasov, M. N. Skvortsov, and S. N. Bagayev: Opt. Lett. (in print, Dec. 2000)
19. See the contribution by Th. Udem et al.: *this edition*, pp. 125–144
20. S. N. Bagayev, A. K. Dmitriyev, and P. V. Pokasov: Laser Phys. **7**, 989 (1997)
21. Presented by S. Bize et al. at the conference *Hydrogen Atom 2* (unpublished)
22. J. Reichert, R. Holzwarth, Th. Udem, and T. W. Hänsch: Opt. Commun. **172**, 59 (1999)
23. M. Niering, R. Holzwarth, J. Reichert, P. Pokasov, T. Udem, M. Weitz, T. W. Hänsch, P. Lemonde, G. Santarelli, M. Abgrall, P. Laurent, C. Salomon, and A. Clairon: Phys. Rev. Lett. **84**, 5496 (2000)
24. V. A. Dzuba, V. V. Flambaum, and J. K. Webb: Phys. Rev. Lett. **82**, 888 (1999)
25. V. A. Dzuba and V. V. Flambaum: Phys. Rev. A **61**, 034502 (2000)
26. V. A. Dzuba and V. V. Flambaum: *this edition*, pp. 564–575
27. T. M. Miller and B. Bederson, in *Adv. in Atomic and Mol. Phys.*, Vol. 13, Eds.: D. R. Bates and B. Bederson (Academic, New York, 1977)
28. N. L. Manakov and V. G. Palchikov: Opt. Spectrosc. (USSR) **46**, 688 (1979)